

The Influence of Gas Generation on Flame Propagation for
Nano-Al Based Energetic Materials

by

Steven W. Dean, B.S.M.E

A Thesis

In

MECHANICAL ENGINEERING

Submitted to the Graduate Faculty
of Texas Tech University in
Partial Fulfillment of
the Requirements for
the Degree of

MASTER OF SCIENCES

IN

MECHANICAL ENGINEERING

Approved

Michelle Pantoya
Chairperson of the Committee

Valery Levitas

Brandon Weeks

Fred Hartmeister
Dean of the Graduate School

December, 2008

Acknowledgments

I would first and foremost like to thank my family for their love and support, and for never doubting me in my desire to continue my education. They have been with me through thick and thin and I attribute much of my success to them.

I would also like to thank my committee members for their help in my research. Dr. Pantoya has been instrumental in my growth as a researcher and as a person, she has taken her role as my advisor past the merely academic realm and I find her input more and more valuable as I continue my trek through academia and life in general. Dr. Levitas has been very helpful with advice and direction, and Dr. Weeks has also been an excellent source of counsel and instruction.

I also gratefully acknowledge support from the Army Research Office contract number W911NF-04-1-0217 and Dr. Ralph Anthenien. I would like to thank William Bender, a high school student participating in the Clark's Scholar summer research program at Texas Tech University, for his aid in conducting the Al+NiO instrumented tube tests. I am also indebted to Shawn Stacy at Texas Tech University for his work on generating predictive data using REAL code, and to Dr. Louisa Hope-Weeks for her aid in the XRD analysis conducted in this work. I would like to thank Dr. Alex Gash at Lawrence Livermore National Laboratory for synthesizing the NiO used in this study as well as providing advice.

Table of Contents

Acknowledgments.....	ii
Abstract.....	v
List of Tables	vi
List of Figures.....	vii
I. Introduction	1
1.1 Overview.....	1
1.2 Propagation Mechanisms in Energetic Composites.....	5
1.3 Gas Generation in Energetic Composites	7
II. Experimental	9
2.1 Sample Preparation	9
2.2. Confined Burns	13
2.3 DSC/TGA Tests	15
2.4 XRD Analysis	17
III. Results.....	18
3.1 Confined Burn Results.....	18
3.2 DSC/TGA Results.....	20
3.3 XRD Results	24

IV. Discussion.....	25
4.1 Instrumented Tube Discussion.....	25
4.2 DSC/TGA Discussion.....	26
4.3 Other Sources of Gas Generation	27
4.4 Implications.....	29
V. Conclusions.....	32
VI. Future Work.....	34
References.....	35
Appendices	
A. Composite Mixing Data.....	38
B.Labeled DSC/TGA Traces	39

Abstract

This study examines the reactions of two nanocomposite thermites, aluminum (Al) with copper oxide (CuO) and aluminum with nickel oxide (NiO). These oxidizers were selected based on their predicted properties: similar adiabatic flame temperatures but significantly opposing gas generation properties. Thermal equilibrium calculations predicted that the Al+CuO would have a high gas output and the Al+NiO would produce little to no gas. Flame propagation rates and peak pressure measurements were taken for both composites at various equivalence ratios using an instrumented flame tube apparatus. Results show that over the range of equivalence ratios studied, Al+CuO had an average propagation rate of 582.9 ± 87.6 m/s, while Al+NiO had an average velocity of 193.7 ± 72.2 m/s. The average peak pressures observed for the reactions were 3.75 ± 0.85 MPa for Al+CuO and 1.68 ± 0.88 MPa for Al+NiO. A DSC/TGA was also used to determine the properties of the composites and reactants under low heating rates. These low heating rate tests indicate that the gas production properties of the composites are highly dependent on heating rate, with both composites experiencing almost no mass loss under slow heating. The results suggest that the melt-dispersion mechanism, which is only engaged at high heating rates, leads to a dispersion of high velocity molten Al clusters that promotes a pressure build-up by inducing a bulk movement of fluid. This mechanism may promote convection without the need for additional gas generation.

List of Tables

1. Powder Properties	9
2. Predicted Reaction Properties (Fischer and Grubelich 1998).....	10
3. Specific information on DSC/TGA traces.	16
4. Summary of Velocity and Peak Pressure Results	19
5. Mixing Data for tests using the Al+CuO composite.....	38
6. Mixing Data for tests using the Al+NiO composite.	38

List of Figures

1. REAL code thermo-chemical simulation for Al+CuO and Al+NiO.	10
2. SEM of mixed Al+CuO composite.....	12
3. SEM of mixed Al+NiO composite.	12
4. Schematic showing high speed camera and data acquisition systems.....	14
5. Still frame images from an Al+CuO test.	15
6. Flame Propagation results for Al+CuO and Al+NiO composites.	18
7. Peak pressure results for Al+CuO and Al+NiO Composites.....	19
8. DSC/TGA trace for 50 nm Al.....	21
9. DSC/TGA trace for CuO.	22
10. DSC/TGA trace for NiO.	22
11. DSC/TGA trace for nm Al + CuO.....	23
12. DSC/TGA trace for nm Al + NiO.....	23
13. XRD graph of intensity versus 2θ for the sol-gel synthesized NiO powder.....	24
14. Schematic of combustion regimes.	31
15. Labeled DSC/TGA trace of nm Al.	39
16. Labeled DSC/TGA trace of CuO.....	40
17. Labeled DSC/TGA trace of NiO.....	41
18. Labeled DSC/TGA trace of nm Al + CuO.	42
19. Labeled DSC/TGA trace of nm Al + NiO.	43

Chapter I

Introduction

1.1 Overview

Thermites are a form of composite energetic material consisting of a metal and a metal oxide (Wang, Munir and Maximov 1993). Thermite reactions are generally characterized by high heats of combustion and high adiabatic flame temperatures. In recent years thermites have seen a significant increase in interest for several applications due to the introduction of their constituent components on the nano-scale. These nano-thermites, sometimes called superthermites or metastable intermolecular (or interstitial) composites (MICs) can have significantly enhanced properties when compared to their micron scale counterparts. These enhanced properties include greatly increased flame propagation rates and gas production, as well as significantly reduced ignition temperatures (Pantoya and Granier 2005). This work focuses on how the confined propagation rates of two nano scaled thermites, Al+CuO and Al+NiO, are influenced by their gas production properties.

Composite energetic materials, including thermites and other metal fueled composites such as Al+PTFE (polytetrafluoroethylene, Teflon ®) amongst others, have many applications such as primer charges in munitions (Giles 2004) or material joining (Varma 2000). A wide array of applications are possible because composite energetics have an extremely large degree of customizability due to their very composite nature: by varying the constituent reactants, such as composition and particle size, the properties of

the mixture can be tailored with respect to gas output, reaction rate, flame temperature, and several other important combustion parameters.

The development of synthesis techniques that allow the production of particles with dimensions on the order of tens of nanometers or less has introduced many new possible applications. These nano-energetic composites have energy densities close to those of their micron-scale brethren, but have power densities several orders of magnitude higher. This increased power density manifests itself as enhanced propagation rates (Bockmon, et al. 2005, Plantier, Pantoya and Gash 2005), peak pressures (Sanders, et al. 2007), and ignition sensitivities (Granier and Pantoya 2004). These enhanced properties can be partially explained by the increased surface area to volume ratio of nano particles which enhances mixture homogeneity and a reduction in the distance between particles. This is not the whole story however: due to the unique properties of nano-scaled materials entirely new reaction mechanisms are possible.

In order to accurately predict the properties of a given mixture it is critical to have a firm grasp of the details of how the mixture's reaction will progress. The composite's customizability can make this prediction difficult because of the many variables involved (i.e. stoichiometry, passivation shell thickness, particle size, etc.). As the reaction dynamics of nano-thermites are not currently well understood, experimentation is often the only recourse to determine a composite's behavior.

Several composites have built up small bodies of literature to describe their properties under various stoichiometric and geometric conditions. Some of these composites include Al+PTFE (Watson, Pantoya and Levitas 2008) (Osborne and Pantoya

2007), Al+MoO₃ (Moore and Pantoya 2006) (Sanders, et al. 2007) (Son, Asay, et al. 2007) (Wilson and Kim 2003), Al+Fe₂O₃ (Plantier, Pantoya and Gash 2005) (Brito, et al. 2007) (Duraes, et al. 2007), and the Al+CuO composite used in this study. Sanders et al. studied the propagation rate and gas generation properties of high density Al+CuO pellets (as well as Al+Bi₂O₃, Al+MoO₃, and Al+WO₃) in a confined geometry similar to the instrumented tube used here (Sanders, et al. 2007). They concluded that propagation rates and peak pressures generated during the reaction are highly dependent on the metallic oxide used. They also showed that the amount of gaseous species produced greatly influences the propagation rate. The effect of diluting the composite with excess Al₂O₃ in the form of added nano-scaled alumina powder was investigated by (Malchi, et al. 2008). It was determined that very small amounts of additional diluting alumina (~5%) can greatly decrease the peak pressure and pressurization rate of the Al+CuO reaction and that higher amounts of alumina (~20%) can cause the propagation rate to no longer be constant, but accelerating. Pressure wave speeds high enough to indicate detonation were reported by Apperson et al. in energetic composites that made use of self-assembled CuO nanorods mixed with nano-scaled aluminum powders (Apperson, et al. 2007). A method for fabricating nano scaled energetic composites from Al and CuO nanorods and nanowires was presented by Shende et al. in work similar to that of Apperson (Shende, et al. 2008). Shende recorded flame propagation rates of 1650 m/s in the nanorod-based composite, 1900 m/s for the nanowire composite, and 2400 m/s for the self-assembled composite. These velocities are all significantly higher than those seen in other publications. Fully dense multilayer foils of CuO_x/Al were studied by (Blobaum, et al.

2003). The composite was formed by sputter deposition, and the structure was confirmed by Auger depth profiling and various transmission electron microscopy (TEM) methods. Results from differential thermal analysis (DTA) show that the foils can react in a highly exothermic manner, with total heats of reaction of -3.9 ± 0.9 kJ/g, similar to that theoretically predicted from chemical equilibrium calculations for Al+CuO.

While the Al+NiO reaction is not as common in the literature as the Al+CuO reaction, there are other reactions of NiO that are of interest to the energetic materials community. Notably it was shown by (Altham, McLain and Schwap 1971) that by doping NiO it is possible to change its reaction temperature with a reducing agent. Doping is the process of adding very small amounts of impurities to a semiconductor in order to change its electrical properties by altering its chemical bonding and crystal lattice. The two types of doping are *n*-doping and *p*-doping; *n*-doping adds negative charge carriers to the crystal lattice of the semiconductor, while *p*-doping adds positive charge carriers. Altham et al. found that *p*-doped NiO would react with a reducing agent at lower temperatures than undoped NiO, while *n*-doped NiO reacted at higher temperatures.

In a similar fashion to composites, several diagnostic techniques have become common due to their ease of use, cost, and the insight they provide to the subject being studied. One such diagnostic is the instrumented flame tube, first developed at Texas Tech University by Bockmon et al. The purpose of this innovative yet simplistic diagnostic test is to characterize the properties of different reactions in terms of modes of energy transfer based on ignition at a single point. This technique's popularity can be seen in the large number of publications that feature its use. Bockmon et al. originally

used the tube apparatus to determine flame propagation rates and pressure data for various Al+MoO₃ composites with different Al particle sizes. They found that propagation rates increase with decreasing particle size and that for tube diameters between 1 mm and 6 mm there is no significant dependence of propagation rate on tube diameter. Apperson et al. made use of an instrumented tube in their study of self-assembled Al+CuO nanocomposites. Malachi et al. used one in their study of the effects of added alumina on the Al+CuO system. Asay et al. used various modifications of the instrumented tube in their studies of MIC ignition characteristics (Asay, et al. 2004). Puszynski et al. used a relatively short tube (~40 mm) to investigate the effects of sealing the ends of the tube on propagation rate of an Al-Fe₂O₃ system (Puszynski, Swiatkiewicz and Bulian 2005). As with all diagnostic techniques, the instrumented flame tube has several limitations including an inability to compare results from various reports due to differences in the geometry of the tube, most notably in the length of the flow development section of the tube.

1.2 Propagation Mechanisms in Energetic Composites

A common metric used to quantify the capabilities of a particular composite is its propagation rate in various geometric configurations, most commonly an open trough and a confined tube. These tests are important as they mimic some useful applications of composites. A confined experiment can be seen as roughly analogous to a primer charge or air bag inflator while an open test could correlate to a welding or cutting application.

For any particular composite, propagation rates are controlled by several factors, namely the heat transfer properties of the composite and its sensitivity to ignition. These

properties can be thought of as the two sides of the “propagation equation”; propagation rates can be increased either by increasing the composites ability to transfer heat and/or by reducing its threshold to ignition. Aluminum fueled nanoscaled thermites are a prime example of how these effects come into play: their heat transfer properties are somewhat inhibited by a much higher mass percentage of alumina compared to micron sized aluminum (in the form of a passivated shell) which is made up for by their much higher ignition sensitivities (Pantoya and Granier 2005).

Heat generated in an energetic composite is transferred as it is through all materials: by conduction, convection, and radiation. Conduction has been found to be the dominant form of transfer in composites whose constituents are on the micron scale, with propagation rates on the order of 0.010 m/s (Brown, Taylor and Tribelhorn 1998). Radiation, while ever-present and able to enhance propagation rates (Son and Brewster 1995), has been shown to be insufficient to cause propagation on its own (Asay, et al. 2004). Asay et al. also showed that in loose packed nanoscaled composites, which are the subject of this study, convection is the main source of heat transfer through the material. The main source of this convective transfer is gas generated by the reaction. There are, however, several composites that are predicted to produce little to no gas. This study investigates one such non-gas generating composite, Al+NiO, and compares it with a known gas generator, Al+CuO; in order to determine what role gas generation effects play in convective heat transfer in the composite.

A fourth method of energy transfer, acoustic/compression, is often listed with the heat transfer modes as a method for flame propagation. This is somewhat misleading as

acoustic/compression energy transfer is more closely related to impact ignition than thermal ignition. The “impact” is caused by a large pressure wave that moves faster than the flame front through the material, causing particles in the composite to strike against each other and potentially leading to ignition. For the studies referenced and the work reported here, thermal ignition up to heating rates of 10^8 K/s does not induce or promote the acoustic/compressive propagation mechanism.

The warnings seen in many publications, this work included, with regard to the danger of synthesizing and handling nano-scaled thermites are a strong testament to their ignition sensitivity. This enhanced sensitivity is caused by the extremely low mass of nano-scaled particles. This low mass means that the particles have essentially no thermal inertia, and so can reach an ignition temperature much more quickly with significantly decreased apparent activation energy than micron scale composites. The small size of the particles also means that they can form almost completely homogeneous mixtures when compared to micron scale composites, leading to separation distances between the fuel and oxidizer falling to nanometer scales.

1.3 Gas Generation in Energetic Composites

Micron-scale thermites are generally considered to be gasless reactions as their products are in a condensed form (Wang, Munir and Maximov 1993). Nano-scale thermites however, have been reported in several studies to have the potential to produce very large amounts of gaseous products (Sanders, et al. 2007) (Watson, Pantoya and Levitas 2008). The gas produced in these reactions is made up of vaporized products

from the reaction. Thus the amount of gas produced by the composite depends largely on the flame temperature of the reaction and the properties of the products.

As gas generation under self propagating conditions is generally measured as a function of pressure in and around the reaction zone, such as in a sealed pressure vessel or the instrumented tube used in this study, other pressure increasing effects can lead to interpretations of gas generation. The most common of these effects is the thermal expansion of interstitial gas in the composite due to the high temperatures reached during the reaction.

Chapter II

Experimental

2.1 Sample Preparation

The composites used in this study were made from commercially obtained powders (Al, CuO) and powder made at Lawrence Livermore National Laboratory (LLNL) using a sol-gel synthesis technique (NiO). Table 1 lists the powders used in this study and some of their properties. Properties for the Al and CuO powders were obtained from their respective manufactures; the particle size and purity for the NiO powder were obtained from x-ray diffraction (XRD) analysis performed at the Department of Chemistry at Texas Tech University. The surface area information was obtained at LLNL. The purity of the NiO powder is a measure of its crystallinity, and not a measure of impurities in the composite. The impurities in the Al powder are composed of non-reactive alumina in the form of an oxidation shell coating the Al particles.

Table 1. Powder Properties

Material	Manufacturer	Particle Size	Surface Area	Morphology	Purity
Aluminum	Novacentrix	50 nm	39.8 m ² /g	Spherical	75%
Copper (II) Oxide	Alfa Aesar	30-50 nm	13 m ² /g	Spherical	98.5%
Nickel (II) Oxide	LLNL	~11 nm	~55 m ² /g	Spherical	~90.5%

These powders were chosen due to their anticipated properties based on data from a thermodynamic simulation program, REAL Code (Timtec, Delaware) and information

from (Fischer and Grubelich 1998). The pertinent Fischer information for stoichiometric conditions is shown below in Table 2.

Table 2. Predicted Reaction Properties (Fischer and Grubelich 1998).

Reaction	Flame Temperature (K)	Gas Production (mol of gas/100 g)	Heat of reaction (-cal/g)
2Al+3CuO	2843	0.5400	974.1
2Al+3NiO	3187	0.0108	822.3

The Al+CuO composite was predicted to have a very high adiabatic flame temperature and high gas production. The Al+NiO reaction was predicted to have a similar flame temperature, but much lower gas production. The REAL code data is shown in Figure 1.

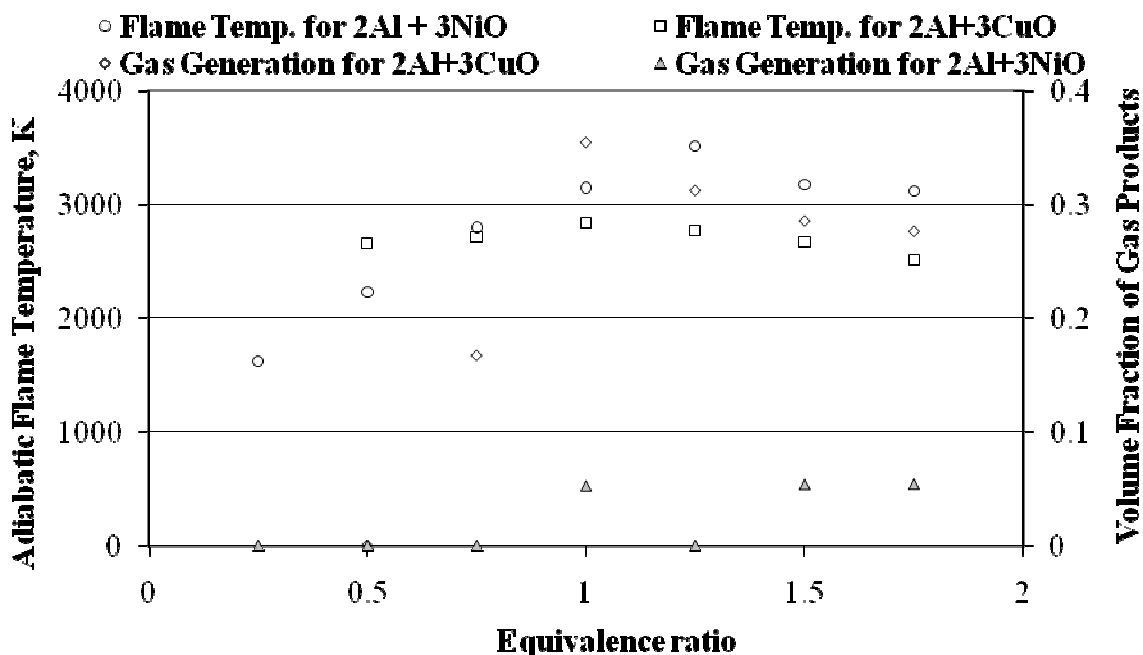


Figure 1. REAL code thermo-chemical simulation for Al+CuO and Al+NiO.

To form the composites a specific amount of each constituent powder was determined based on the desired equivalence ratio (ER) calculated from Equation (1).

$$ER = \frac{F/O_{act}}{F/O_{stn}} \quad (1)$$

The numerator refers to the actual fuel to oxide ratio on a mass basis. The denominator refers to the calculated stoichiometric ratio. The chemical reactions used to determine the stoichiometric ratios are shown below in Equations (2) and (3). The purity of the Al powder was factored into this calculation, the oxidizers were assumed to have a purity of 100%.



The component powders were combined to form roughly 500 mg of composite. This amount was chosen both for safety reasons and because it was slightly more than the amount required to fill a tube. A small amount of hexane (approx 50 mL) was added to the powder to form a solution. A Misonix Sonicator 3000 ultrasonic probe mixer was used in order to break apart agglomerates that may have formed in the solution. The solution was sonicated for 120 seconds with pulses of 10 seconds on, then 10 seconds off. The low duty cycle was chosen to give the solution time to cool between on cycles in order to reduce any thermal damage to the particles.

After mixing, the solution was poured into a glass dish and placed under a fume hood on a hot plate set to 50 °C to allow the hexane to evaporate. Time on the hot plate

was limited to just after the last of the hexane had evaporated (approximately 10 minutes) in order to limit oxidation of the aluminum particles. For safety purposes the dish was then placed in a glove box and a grounded metal brush was used to remove the dried powder. These powders were found to not be as sensitive to accidental ignition as other known composites (such as Al+MoO₃), but great care was still taken to avoid any potential hazards. Scanning electron micrographs (SEMs) of the mixed powders are shown in Figures 2 and 3. These micrographs show that the powders are relatively homogeneous and give a rough indication of the size distributions of the composites.

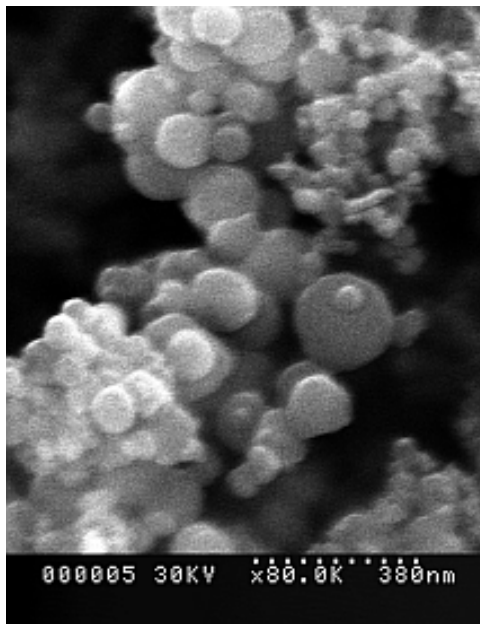


Figure 2. SEM of mixed Al+CuO composite.

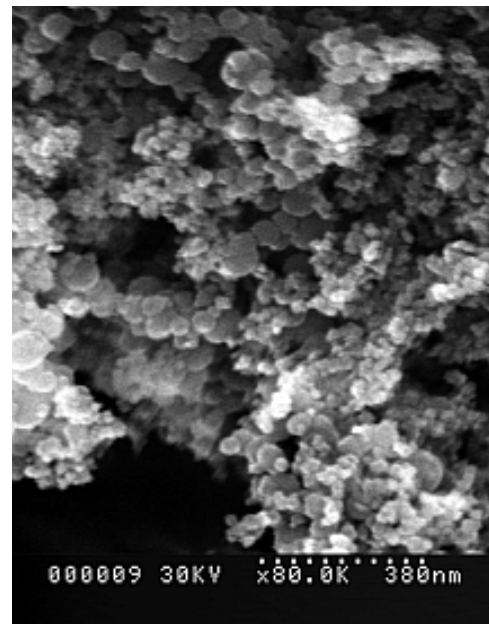


Figure 3. SEM of mixed Al+NiO composite.

2.2. Confined Burns

An instrumented tube was used in this study to gather data on flame propagation rates and pressures, similar to the “Bockmon Tube” reported in (Bockmon, et al. 2005). The tube is 100 mm long, with an outer diameter of 25.4 mm and an inner diameter of 3.18 mm. Both ends of the tube were sealed with vinyl adhesive tape; one end had a small length of Nichrome® wire (80% Ni, 20% Cr; Omega Engineering, Inc.) bent into a u-shape positioned to serve as an ignition source. Four 0.19 mm diameter holes were drilled perpendicular to the center of the tube to facilitate the acquisition of pressure data along the length of the tube.

Once the composite powder had been prepared, it was slowly loaded into the top of an acrylic tube with the bottom end sealed with adhesive vinyl tape containing the ignition mechanism. Blockages would form in the tube as the powder was added due to interactions between the powder and machined tube wall, so the tube would be gently tapped during loading to make sure the tube filled completely. After the tube was fully loaded, the other end was sealed in a similar manner and the tube was placed horizontally on a vibrating pad in order reduce density gradients induced by tapping.

Once the tube was filled with powder, it was loaded into a steel block 50.4 mm square and 102 mm long, with a 25.4 mm diameter hole drilled to accept the tube. The block also had a 25 mm by 85 mm window milled into its side to allow for the acquisition of flame propagation information by the use of a Phantom 7 (Vision Research) high speed digital camera set to record at 51,000 frames per second. The small holes in the tube were aligned with four PCB Peizotronics model 113A22 piezoelectric pressure

sensors mounted on the block. The steel block was then placed into an experimental chamber and aligned with the high speed camera, the Nichrome wire in the tube was attached to a 15V AC power supply, and the chamber was sealed. The pressure in the chamber was then lowered to approximately 63 kPa, the limit of the diaphragm based vacuum system, then backfilled with argon up to atmospheric pressure (approximately 100 kPa). The experimental setup is outlined in Figure 4.

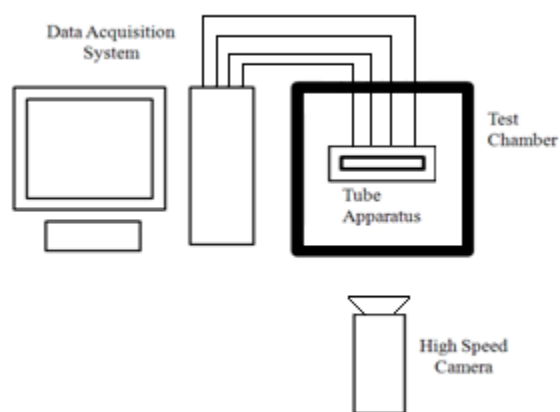


Figure 4. Schematic showing high speed camera and data acquisition systems.

To initiate a test first the pressure sensor data acquisition system was engaged through Labview 8.0 (National Instruments), then the AC transformer attached to the Nichrome wire was turned on which would immediately initiated the reaction. Once the reaction had run to completion the high speed camera was post-triggered to record the previous few seconds of footage. Figure 5 shows a series still images taken from an Al+CuO test at an ER of 2.5. The vertical lines in the image are from hot gasses propagating through the small holes used to collect pressure data.

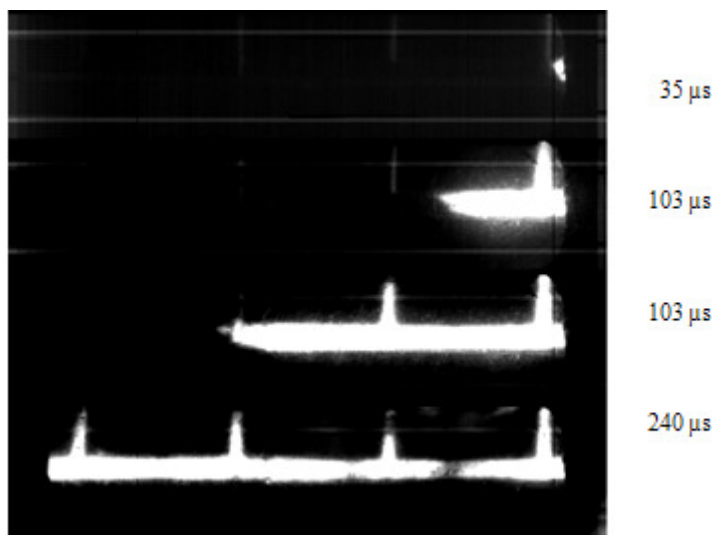


Figure 5. Still frame images from an Al+CuO test.

2.3 DSC/TGA Tests

A differential scanning calorimeter (DSC) measures the difference in the heat flow required to keep a reference and sample at the same temperature. It is commonly used to determine the temperature of phase changes a material may undergo, as well as the amount of energy given off by a reaction. It can also be used to determine the onset temperatures of phase changes and reactions. Heating rates in DSCs are usually between 5 and 50 °C per minute.

A thermo gravimetric analyzer (TGA) is a sensitive balance that measures mass change as a function of temperature. A TGA can accurately show at what temperature a material loses or gains mass, as well as showing the amount of mass lost. This mass change can then be used to determine important reaction parameters. For instance, a mass loss could correspond to gas production, while a mass gain could indicate oxidation. By combining a DSC and TGA in the same instrument it is possible to accurately determine how a reaction progresses as a function of temperature. Several researchers

have used DSC/TGAs to study energetic materials. A study was made of the phase transformations of the alumina shell that coats aluminum powders at high temperatures by (Trunov, et al. 2005). Trunov identified several stages that the alumina shell undergoes during heating, starting with shell growth, and followed by several phase transformations. Analysis was also conducted by (Umbrajkar, Schoenitz and Dreizin 2006) using a DSC/TGA to study Al+CuO composites.

In this study a Netzsch STA 409 PC DSC/TGA was used to conduct tests on both the individual reactants and composites. The DSC/TGA was purged with Ar during the tests; the purge gas flow rate was 17 ml/min while the balance protection flow rate was 42.5 ml/min. All samples were run in Pt crucibles with alumina liners. The samples were heated either to 1000 °C or 1400 °C. Details of the tests are shown in Table 3.

Table 3. Specific information on DSC/TGA traces.

Material	Sample Mass (mg)	Heating Rate (°C/min)	Max Temperature (°C)	Atmosphere
50 nm Al	12.68	10	1000	Ar
3-4.5 μm Al	15.05	10	1000	Ar
NiO	8.58	10	1000	Ar
CuO	51.47	10	1400	Ar
nm Al+CuO	2.44	10	1400	Ar
nm Al+NiO	3.13	10	1400	Ar
μm Al+CuO	4.13	10	1400	Ar
μm Al+NiO	3.54	10	1400	Ar

2.4 XRD Analysis

In order to determine additional properties of the NiO powder, such as crystallinity and particle size, powder x-ray diffraction was performed using a Rigaku Ultima III powder XRD operating at 40 kV and 44 mA using copper K_{α} radiation.

Chapter III

Results

3.1 Confined Burn Results

Figure 6 details the flame propagation results of these tests, as determined by high speed photography. Each data point corresponds to a single test at that equivalence ratio. The average velocity observed over the range of stoichiometries tested for the Al+CuO composite is 582.91 ± 87.6 m/s, where the uncertainty is one standard deviation. The average velocity of the Al+NiO composite between equivalence ratios of 1.5 and 2.7 was 193.7 ± 72.21 m/s. Speeds from equivalence ratios lower than 1.5 were not taken into consideration as it appears that these values appear to be the limits of flammability of the composite.

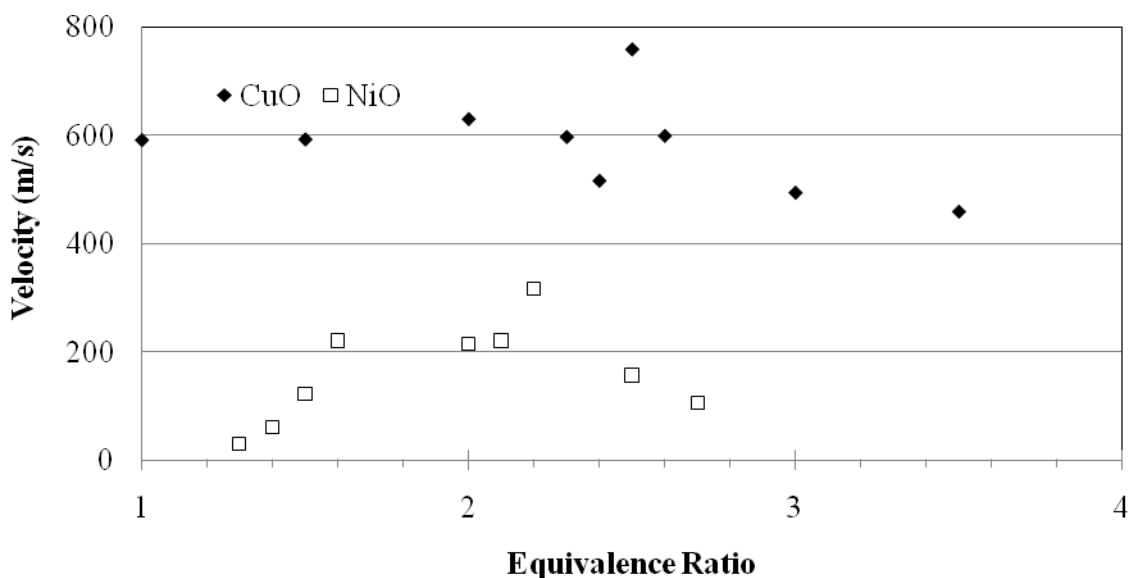


Figure 6. Flame Propagation results for Al+CuO and Al+NiO composites.

Figure 7 shows the observed peak pressures, as determined by piezoelectric pressure sensors. The average pressure observed for the Al+CuO composite over the

range of equivalence ratios tested was 3.74 ± 0.85 MPa. The Al+NiO composite had an average pressure of 1.68 ± 0.88 MPa. As in the velocity measurements, data from equivalence ratios below 1.5 were not included in these calculations.

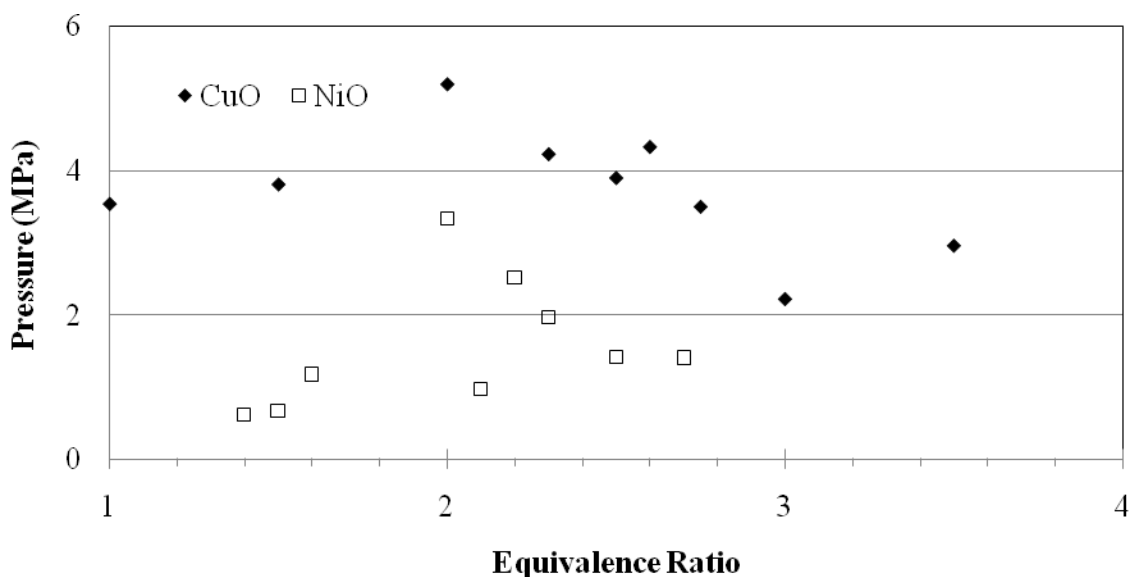


Figure 7. Peak pressure results for Al+CuO and Al+NiO Composites.

These velocity and pressure results are summarized in Table 4, along with the pressure rise time, which is defined as the time it takes the pressure signal to go from 5% to 95% of the peak pressure value, this data was collected from the fourth pressure sensor as it had the most repeatable results. The uncertainty corresponds to one standard deviation from the average value.

Table 4. Summary of Velocity and Peak Pressure Results

Composite	Velocity (m/s)	Peak Pressure (MPa)	Pressure Rise Time ($\times 10^{-4}$ s)
Al+CuO	582.9 ± 87.6	3.74 ± 0.85	1.94 ± 1.74
Al+NiO	193.7 ± 72.2	1.68 ± 0.88	2.78 ± 1.82

3.2 DSC/TGA Results

The thermal analysis from DSC/TGA tests are shown in Figures 8 to 12. The solid line is the DSC signal, while the dotted line is the TGA signal. Larger images, with onset temperatures and percent mass changes shown, can be found in the appendix in Figures 15 to 20. Many of the traces show mass losses and harmonic DSC behavior at low traces; these are thought to be artifacts of the measurement technique, and not actual phenomena.

Figure 8 shows the DSC/TGA trace for the 50 nm Al used in this experiment. The trace initially shows an exotherm with an onset temperature of 548 °C. This exotherm is most likely caused by limited oxidation of the Al powder with trace amounts of oxygen in the argon used to purge the DSC during measurement. The melting endotherm is very apparent; it has an onset temperature of approximately 653 °C. This is slightly lower than the bulk melting temperature of Al which is commonly seen in nanoscaled powders, it is caused by a large increase in the number of surface atoms in materials on the nanoscale, known as the Gibbs-Thompson effect (Gibbs 1948). The effect is generally not as significant in Al as it is in other nanoscaled materials as the passivation layer of alumina that coats the aluminum particles contains the particle and allows pressure to build inside the core, causing an increase in melting temperature. The initial mass loss between 100 °C and 300 °C may be caused by the loss of water trapped in the powder during storage. The mass gain observed at temperatures over 300 °C could be due to the previously mentioned limited oxidation that occurs during the test.

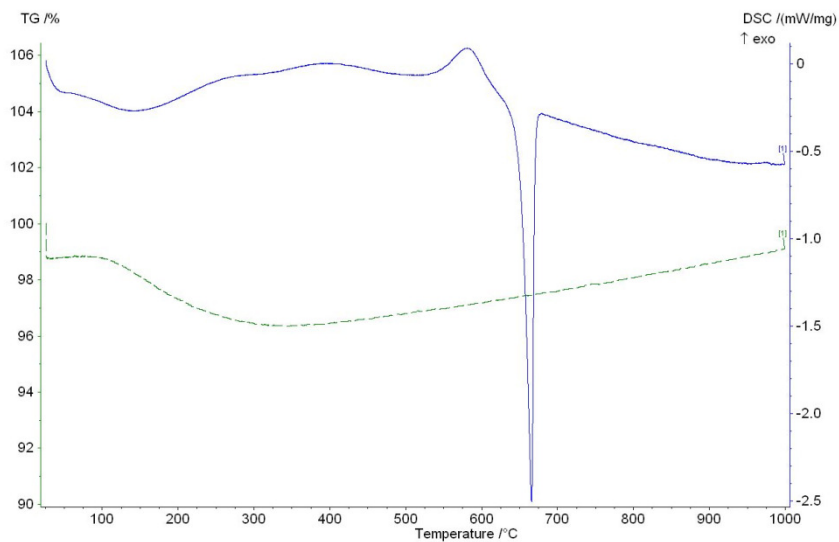


Figure 8. DSC/TGA trace for 50 nm Al.

Figure 9 shows the DSC/TGA traces for CuO. There are several small endotherms throughout the curve that may be caused by small impurities in the CuO powder. The first large endotherm at 1015 °C is accompanied by a mass loss of 9.3%. This corresponds to the melting of the CuO and a loss of some oxygen. The second large endotherm corresponds to copper melting.

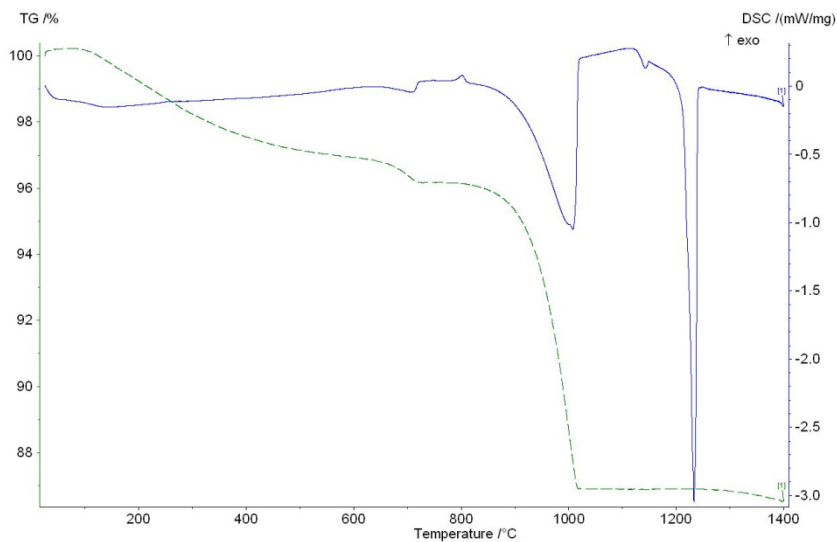


Figure 9. DSC/TGA trace for CuO.

Figure 10 shows the DSC trace for the sol-gel synthesized NiO. It is accompanied by a steady mass loss that may be attributed to the burning off of solvents left over from the sol-gel process.

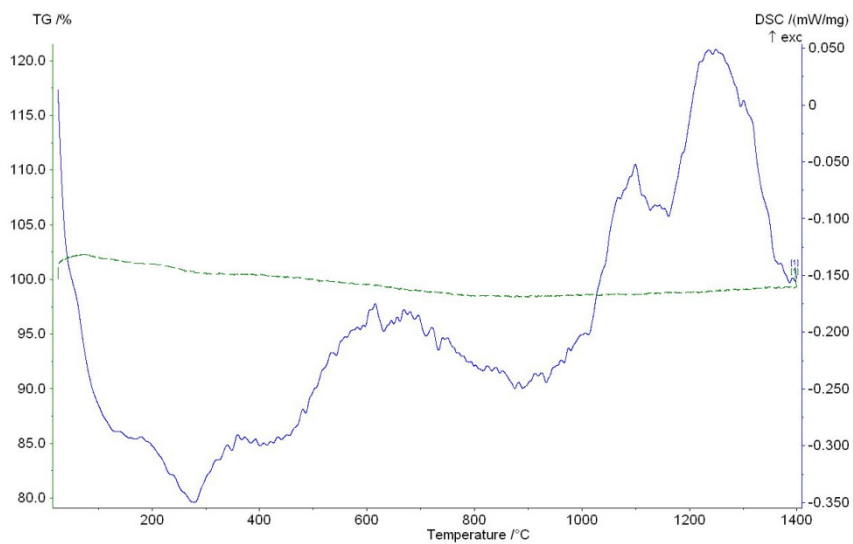


Figure 10. DSC/TGA trace for NiO.

The reaction between 50 nm Al and CuO is shown in Figure 11. The exothermic reaction begins at 522 °C.

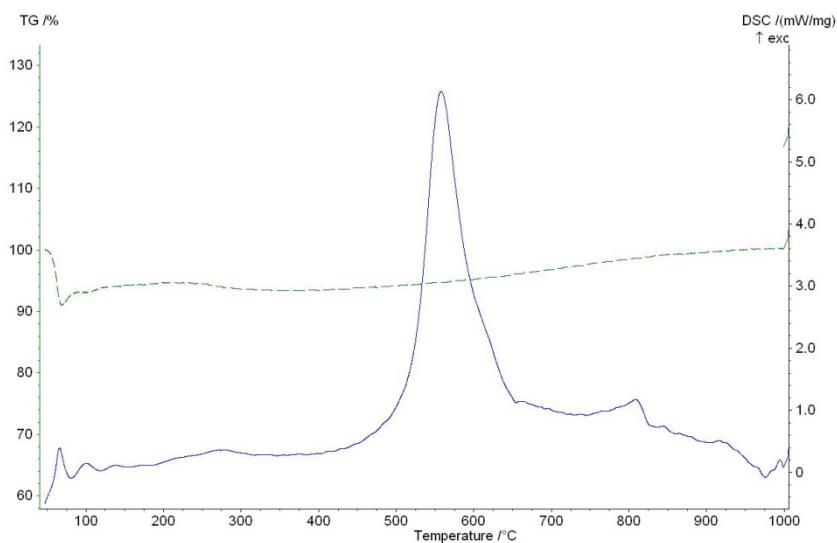


Figure 11. DSC/TGA trace for nm Al + CuO.

Figure 12 shows the reaction of 50 nm Al and NiO. The graph shows what may be a two stage reaction, with the first exotherm at 501 °C while the second starts at 645 °C.

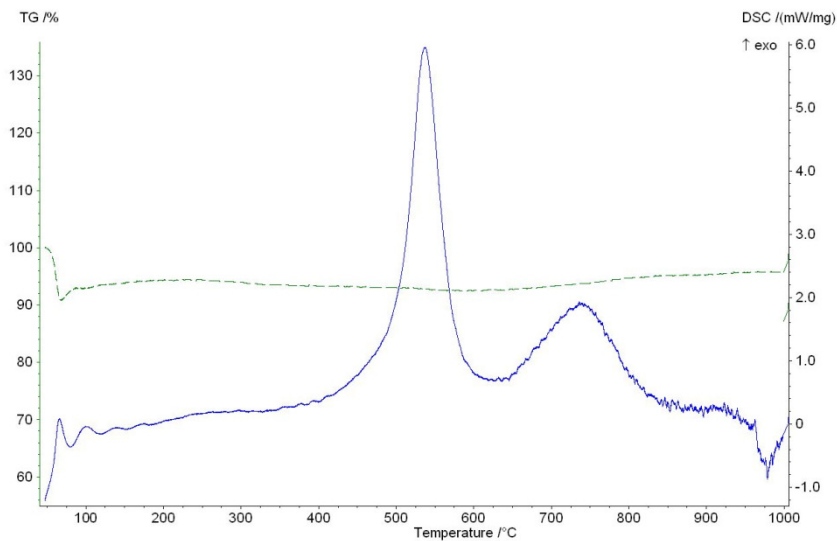


Figure 12. DSC/TGA trace for nm Al + NiO.

3.3 XRD Results

The XRD analysis performed on the NiO sample showed that it was largely crystalline with some amorphousness present. The average particle size was between 11 and 14 nm. The d-spacing of the NiO was slightly larger than that for bulk NiO. No significant contaminants were found in the powder. The intensity- 2θ graph is shown in Figure 13.

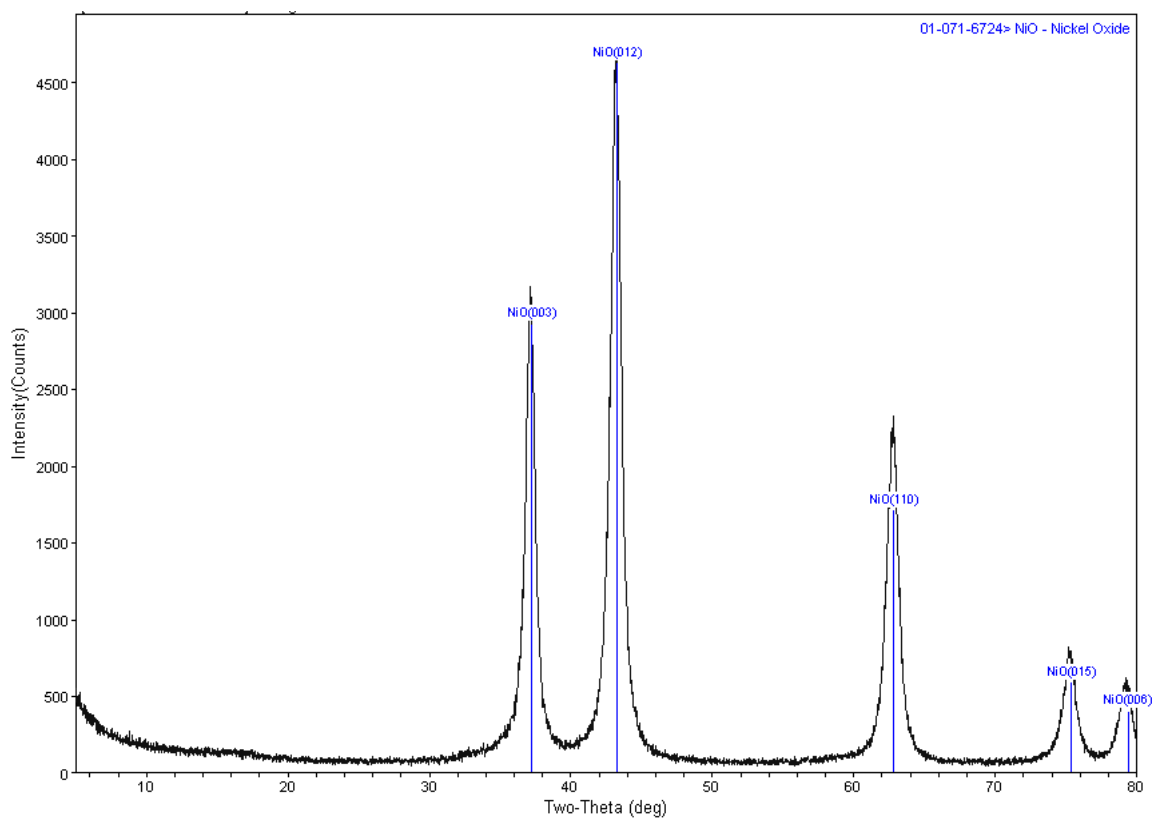


Figure 13. XRD graph of intensity versus 2θ for the sol-gel synthesized NiO powder.

Chapter IV

Discussion

4.1 Instrumented Tube Discussion

The Al+CuO composite had propagation rates and peak pressures approximately twice that of the Al+NiO. This is an unexpected result since the Al+NiO was predicted to have no appreciable gas generation. One explanation for this result is that the Al+NiO composite does not generate gas in the normal sense, i.e. as a product of combustion. Rather the high pressures recorded may be caused by the bulk movement of fluid brought about by a melt dispersion mechanism. This new mechanism for nano-Al particle combustion has been recently introduced for fast (high heating rate) oxidation (Levitas, Asay, et al. 2006) (Levitas, Asay, et al. 2007) (Levitas, Pantoya and Dikici 2008). The mechanism for reaction is not limited by diffusion through an oxide shell but rather dispersion of fast moving molten Al clusters that have broken away from the fuel particle via an unloading pressure wave caused by the spallation of the alumina shell surrounding the molten Al core. The flow induced by the melt dispersion mechanism may contribute toward the high peak pressures measured in Fig. 7. In this way, the mode of propagation can be described as a dispersively driven convective wave.

Diffusion through the Al particles alumina shell is not likely the dominant reaction mechanism considering the pressure rise time of the reaction. The pressure rise time is the time it takes the pressure to rise from 5% to 95% of the peak value (Watson, Pantoya and Levitas 2008). This rise time approximates the timescale of the reaction

itself. The distance through which diffusion occurs during this time can be approximated using Equation 4 (Watson, Pantoya and Levitas 2008).

$$l_d = 2\sqrt{D\tau} \quad (4)$$

Here l_d is the distance through which diffusion will occur, D is the diffusivity of oxygen through alpha-alumina at 800 °C which is approximately 10^{-19} cm²/s (Bergsmark, Simensen and Kofstad 1989), and τ is the order of magnitude for the reaction time which is 10^{-4} s for the experiments conducted here. Solving Equation (4) yields a diffusion distance of approximately 6×10^{-13} m, which is smaller than the atomic radius of an aluminum atom (approximately 125×10^{-12} m, (Slater 1964)). As this distance is far smaller than the thickness of the alumina shell coating the fuel particles, there must be a mechanism other than diffusion through the oxide shell which is controlling the reaction.

Other explanations for the high peak pressures seen in the Al+NiO composite may involve the composition and phase of the NiO material. The d-spacing results from XRD analysis suggest that the material may be in a metastable phase that may readily decompose into Ni and O when exposed to high temperatures. Under the slow heating rates of the DSC/TGA, however, no decomposition was observed.

4.2 DSC/TGA Discussion

The DSC/TGA tests conducted in this study help to confirm the results of the instrumented flame tube experiments. The DSC/TGA traces of the constituent powders show that they have no significant impurities. Both nano-scaled reactions show no significant mass change, although they do exhibit large exothermic activity. This was expected as under low heating rates diffusion through the passivation shell best describes

the reaction mechanism. It is only at high heating rates that the melt dispersion mechanism is engaged, this mechanism is what leads to the proposed dispersively driven convective wave which induces the high peak pressures observed in the Al+NiO composite.

4.3 Other Sources of Gas Generation

Gas generation is often experimentally determined by measuring a pressure rise during the reaction. The main contributor to this rise is the gas generated by the reaction, but contributions are also made by the expansion of gas in the tube due to the reaction's high temperature and by dynamic effects caused by the movement of gases in the tube. A first order approximation of the pressure rise caused by the expansion of interstitial gasses in the tube can be made by using the Ideal Gas Law, shown in Equation 5.

$$P = \frac{nRT}{V} \quad (5)$$

Where P is the pressure, V is the volume of the vessel, n is the moles of gas in the vessel, R is the universal gas constant, and T is the temperature of the reaction. The moles of interstitial gas present, n , are determined in this approximation from assuming that the tube is a closed system and knowing the free volume of the test vessel, that is the volume of the tube not taken up by the composite. The temperature can be conservatively estimated as the adiabatic flame temperature of the reaction and the volume of the vessel is known.

Based on these assumptions, a pressure rise of 1.12 MPa was calculated for a stoichiometric Al+NiO composite and 1.0 MPa for the Al+CuO composite. The average

observed values for both composites were 3.74 ± 0.85 MPa for Al+CuO and 1.68 ± 0.88 MPa, for Al+NiO.

This Ideal Gas Law analysis is only an approximation of the effects of expanding interstitial gas on pressure measurements. It assumes, first and foremost, that the gasses within the tube behave as ideal gasses. The ideal gas assumption is most accurate for gasses at high temperatures and low pressures, whereas in the tube high temperatures and high pressures are present. Another assumption is that the gas is at equilibrium at the predicted adiabatic flame temperature of the composite, which is inaccurate. The conditions within the tube are extremely dynamic. This rapid movement of gas within the tube could cause which could contribute to a measured pressure increase.

A thermodynamic equilibrium program, REAL Code, was used to calculate the thermal-physical properties of the materials in this study. Results show that the reaction flame temperature is highest when the fuel/oxidizer ratio is near stoichiometric conditions. For the Al+NiO composite the pressures observed in the instrumented tube tests show that the pressures near this ratio are lower than those predicted by the Ideal Gas Law, even though the measurements include gas generated by the composite during the reaction. For the Al+CuO composite the observed pressures are significantly higher than those predicted by this analysis, though the adiabatic flame temperature for this reaction is lower than that for the Al+NiO reaction. This analysis suggests that the measured peak pressures are not highly dependent on the thermal expansion of gasses in the instrumented tube during the reaction, but rather on the gas production of the composite.

4.4 Implications

The two series of tests in this study, the instrumented tube and the DSC/TGA, give insight into two different facets of the Al+CuO and Al+NiO reactions behavior. The tube tests lend information about the reactions when heated at a relatively high rate, while the DSC/TGA tests show how the reactants and composites behave under extremely low heating rates. The large difference in reaction behavior between the two tests shows that these reactions are strongly dependent on heating rate.

The high heating rates generated in the confined tube led to fast reaction rates (self propagating) and high pressure measurements. The low heating rates used in the DSC/TGA experiments caused slow equilibrium reactions (not self propagating) and very low gas generation, as evidenced by the low mass loss observed during the reactions in Figures 8 through 12. These tests appear to lead to the conclusion that the gas generating ability of these materials is greatly enhanced by high heating rates, and significantly stifled by low heating rates.

This supports the hypothesis that the gas generation observed via peak pressures in the Al+NiO composite is a physically driven effect that depends on the spallation of the alumina shell coating the Al fuel caused by the melt dispersion mechanism. This is in contrast to the Al+CuO reaction, where the gas generation is caused by the physically driven spallation mechanism as well as the thermodynamically driven phase changes of the reactions products. These results suggest that the aerosolized molten Al droplets resulting from the melt dispersion mechanism may contribute to enhancing convective propagation in a flame tube.

Flame propagation can be characterized as a series of ignition sites. In this study the ignition sensitivity of both reactions is largely a function of the nano-scale Al powder, which is the same for both the Al+CuO and Al+NiO reactions. Along these lines ignition sensitivity is a controlled parameter in this study while gas generation from the reaction is the primary dependant variable. The reactions in a flame tube were observed to produce similar orders of magnitude velocity and pressure such that the reaction gas generation may not influence flame speed and pressure for nano metal-metal oxide in a flame tube. Instead, velocity and pressure measurements may be more closely related to the mechanism of nano-Al reaction, i.e. the melt dispersion mechanism. In this way a dispersively driven convective mode produces the measured high velocity and pressure.

Figure 14 shows a graph of some currently known combustion regimes, highlighting the dependence of propagation rate on particle size. The schematic shows the mechanisms and modes of propagation, as well as some examples of composites that exhibit that behavior. The velocity ranges given in the schematic are exclusive to the instrumented tube diagnostic described here, with the exception of the monomolecular bond breaking entry. An entry for nano-scale composites that do not normally exhibit gas generation has been added to the graph between the diffusion regime that controls micron scale reactions and the dispersion with gas generation regime that describes reaction behavior at the nano-scale for gas producing composites.

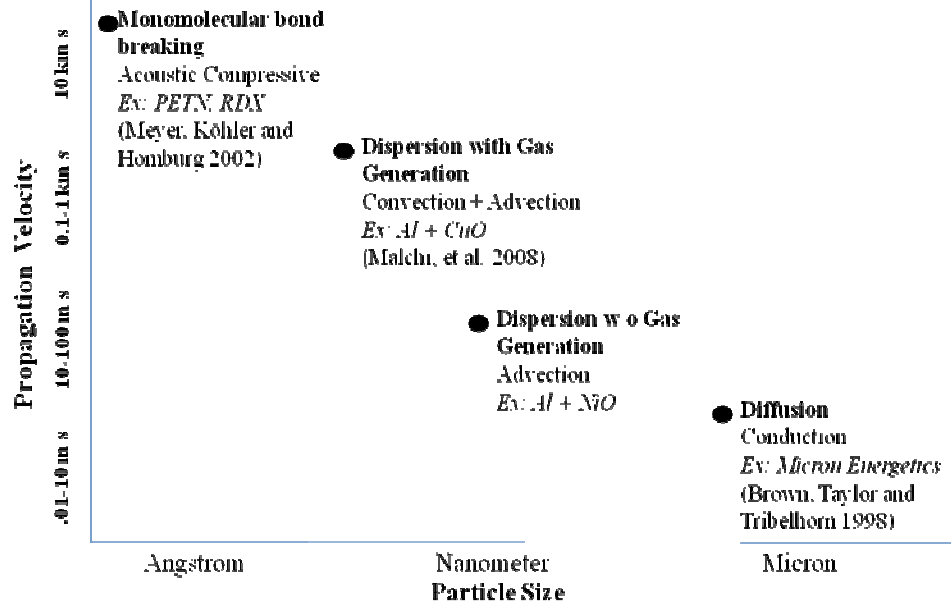


Figure 14. Schematic of combustion regimes.

Chapter V

Conclusions

A series of tests were conducted on two different nanoscaled energetic composites, Al+CuO and Al+NiO, at different equivalence ratios. The Al and CuO were obtained from commercial sources; the NiO was synthesized at LLNL using a sol-gel technique. Using an instrumented flame tube apparatus average values for flame propagation rate and peak pressure were determined for a range of equivalence ratios. Average velocities recorded for the Al+CuO and Al+NiO were 582.9 ± 87.6 m/s and 205.5 ± 71.2 m/s, respectively. Average peak pressures recorded were 3.75 ± 0.85 MPa for the Al+CuO and 1.83 ± 0.89 MPa for the Al+NiO. The Al+NiO flame speed and peak pressure were unexpected as it was predicted to evolve almost no gas and have a very low flame propagation rate. Slow heating experiments were also conducted on the composites and reactants using a DSC/TGA. These tests showed that the reactants were pure and that the composites produce little to no gas under low heating rates.

The large amount of gas generated by the Al+NiO reaction under high heating rates was potentially explained as a forced convective wave created by the bulk movement of aerosolized molten Al clusters released during the rupture of aluminum particles brought about by the melt dispersion mechanism.

The gas generation properties for both reactions were determined to be significantly dependant on heating rate. When heated quickly in the instrumented flame tube significant peak pressures were noted in both composites, while slow heating in the DSC/TGA led to no appreciable mass loss.

This is the first study to show that composites that had previously been predicted to have no significant gas production can in fact be large gas generators due to new reaction mechanisms possible at the nano-scale under high heating rates. As shown in the schematic in Figure 14, this newly proposed reaction mechanism can generate propagation rates comparable to those of gas producing nano-scaled composites, and far in excess of micron scaled composites.

Chapter VI

Future Work

The NiO powder used in the experiment was synthesized in very small quantities at LLNL by Dr. Alex Gash. The quantity available for study was small enough that a repeatability study could not be done due to a lack of material for testing. In the future should more material become available then more tests of the Al+NiO composite should be carried out to confirm the results observed in this study.

There are many tests used to determine the properties of an energetic material under high heating rates. Of these three of the most common are confined tube, open tray, and sealed pressure vessel (a “Parr Bomb”). This study involved the confined tube test, so future studies focused on other material configurations could prove beneficial.

References

- Altham, J. A., J. H. McLain, and G. M. Schwap. "The Reactivity of Nickel Oxide." *Zeitschrift fur physikalische chemie neue folge*, 1971: 139-145.
- Apperson, S., et al. "Generation of fast propagating combustion and shock waves with copper oxide/aluminum nanothermite composites." *Applied Physics Letters* 91 2007.
- Asay, Blaine W., Steven F. Son, James R. Busse, and David M. Oschwald. "Ignition Characteristics of Metastable Intermolecular Composites." *Propellants, Explosives, Pyrotechnics*, 2004: 216-219.
- Bergsmark, E., C. J. Simensen, and P. Kofstad. "Oxidation of Molten Aluminum." *Bergsmark, E., Simensen, C.J., & Kofstad, P. (1989). Oxidation of molten aluminum. Materials Science & Engineering A: Structural Materials: Properties, Microstructure and Processing*, 1989: 91-95.
- Blobaum, K. J., M. E. Reiss, J. M. Plitzko Lawrence, and T. P. Weihs. "Deposition and characterization of a self-propagating CuOx/Al thermite reaction in a multilayer foil geometry." *Journal of Applied Physics*, 2003: 2915-2922.
- Bockmon, B. S., M. L. Pantoya, S. F. Son, B. W. Asay, and J. T. Mang. "Combustion velocities and propagation mechanisms of metastable interstitial composites." *Journal of Applied Physics*, 2005.
- Brito, Paulo, Luisa Duraes, Jose Campos, and Antonio Portugal. "Simulation of Fe₂O₃/Al combustion: Sensitivity analysis." *Chemical Engineering Science*, 2007: 5078-5083.
- Brown, M. E., S. J. Taylor, and M. J. Tribelhorn. "Fuel - Oxidant Particle Contact in Binary Pyrotechnic Reactions." *Propellants, Explosives, Pyrotechnics*, 1998: 320-327.
- Duraes, Luisa, Benilde F. O. Costa, Regina Santos, Antonio Correia, Jose Campos, and Antonio Portugal. "Fe₂O₃/aluminum thermite reaction intermediate and final products characterization." *Materials Science & Engineering*, 2007: 199-210.
- Fischer, S. H., and M. C. Grubelich. "Theoretical Energy Release of Thermites, Intermetallics and Combustion Metals." *24th International Pyrotechnics Seminar*. Monterey, CA, 1998.
- Gibbs, J.W. *The collected works of J. Willard Gibbs*. New Haven: Yale University Press, 1948.
- Giles, Jim. "Green Explosives: Collateral Damage." *Nature*, 2004: 580-581.

- Granier, J. John, and Michelle L. Pantoya. "Laser ignition of nanocomposite thermites." *Combustion and Flame*, 138 2004: 373-383.
- Levitas, Valery I., Blaine W. Asay, Steven F. Son, and Michelle Pantoya. "Mechanochemical mechanism for fast reaction of metastable intermolecular composites based on disperion of liquid metal." *Journal of Applied Physics*, 101 2007.
- Levitas, Valery I., Blaine W. Asay, Steven F. Son, and Michelle Pantoya. "Melt disperion mechanism for fast reaction of nanothermites." *Applied Physics Letters*, 89 2006.
- Levitas, Valery I., Michelle L. Pantoya, and Birce Dikici. "Melt dispersion versus diffusive oxidation mechanism for aluminum nanoparticles: Critial experiments and controlling parameters." *Applied Physics Letters* 92 (2008).
- Malchi, J. Y., T. J. Foley, S. F. Son, and R. A. Yetter. "The effect of added Al₂O₃ on the propagation behavior of an Al/CuO nano-scale thermite." *Journal of Propulsion and Power*, 2008: 1278-1294.
- Meyer, R., J. Köhler, and A. Homburg. *Explosives*. 5th. Weinheim: Wiley-VCH, 2002.
- Moore, K. and Pantoya, M. L. "Combustion Effects of Environmentally Altered Molybdenum Trioxide Nanocomposites." *Propellants, Explosives, Pyrotechnics*, 2006.
- Osborne, Dustin T., and Michelle L. Pantoya. "Effect of Al Particle Soze on the Thermal Degradation of Al/Teflon Mixtures." *Combustion Science and Technology*, 2007: 1467-1480.
- Pantoya, Michelle L., and John J. Granier. "Combustion Behavior of Highly Energetic Thermites: Nano verses Micron Composites." *Propellants, Explosives, Pyrotechnics*, 2005: 53-62.
- Plantier, K. B., M. L. Pantoya, and A. E. Gash. "Combustion wave speeds of nanocomposite Al/Fe₂O₃: the effects of Fe₂O₃ particle synthesis technicque." *Combustion and Flame*, 140 2005: 299-309.
- Puszynski, Jan A., Jacek J. Swiatkiewicz, and Chris J. Bulian. "Investigation of Reaction Mechanisms and Combustion Characteristics of." *AICHE Annual Meeting*. Cincinnati, OH: AIChE, 2005.
- Sanders, Eric V., Blaine W. Asay, Timothy J. Foley, Bryce C. Tappan, Adam N. Pacheco, and Steven F. Son. "Reaction Propagation of Four Nanoscale Energetic Composites (Al/MoO₃, Al/WO₃, Al/CuO, and Bi₂O₃)." *Journal of Propulsion and Power*, 23 2007.

- Shende, R., et al. "Nanoenergetic Composites of CuO Nanorods, Nanowires, and Al-Nanoparticles." *Propellants, Explosives, Pyrotechnics*, 2008: 122-130.
- Slater, J. C. "Atomic Radii in Crystals." *The Journal of Chemical Physics*, 1964: 3199-3204.
- Son, S. F., and M. Q. Brewster. "Radiation-Augmented Combustion of Homogeneous Solids." *Combustion Science and Technology*, 1995: 127-154.
- Son, S. F., B. W. Asay, T. J. Foley, R. A. Yetter, M. H. Wu, and G. A. Risha. "Combustion of Nanoscale Al/MoO₃ Thermite in Microchannels." *Journal of Propulsion and Power*, 2007: 715-721.
- Trunov, M. A., M. Schoenitz, X. Zhu, and E. L. Dreizin. "Effect of polymorphic phase transformations in Al₂O₃ film on oxidation kinetics of aluminum powders." *Combustion and Flame*, 2005: 310-318.
- Umbrajkar, S. M., M. Schoenitz, and E. L. Dreizin. "Exothermic reactions in Al-CuO nanocomposites." *Thermochimica Acta*, 2006: 34-43.
- Varma, Arvind. "Form From Fire." *Scientific American*, 2000: 58-61.
- Wang, L. L., Z. A. Munir, and Y. M. Maximov. "Thermite reactions: Their utilization in the synthesis and processing of materials." *Journal of Materials Science*, 28 1993: 3693-3708.
- Watson, K. W., M. L. Pantoya, and V. I. Levitas. "Fast reactions with nano and micrometer aluminum: A study on oxidation versus fluorination." *Combustion and Flame*, August 2008.
- Wilson, E. Dennis, and Kyoungjin Kim. "A Simplified Model for the Combustion of Al/MoO₃ Nanocomposite Thermites." *39th AIAA/ASME/SAE/ASEE Joint Propulsion Conference and Exhibit*. Huntsville, AL: American Institute of Aeronautics and Astronautics, 2003.

Appendix A

Composite Mixing Data

Table 5. Mixing Data for tests using the Al+CuO composite.

ER	Al (mg)	CuO (mg)	Total Mass (mg)
1	103	350	453
1.5	132	300	432
2	162	275	437
2.5	184	250	434
3	375	425	800
3.5	412	400	812
2.3	169	250	419
2.75	186	230	416
2.4	166	235	401
2.6	176	230	406

Table 6. Mixing Data for tests using the Al+NiO composite.

ER	Al (mg)	NiO (mg)	Total (mg)
1.3	117	280	397
1.34	150	465	615
1.4	126	280	406
1.45	130	280	410
1.5	135	280	415
1.6	139	270	409
2	161	250	411
2.1	162	240	402
2.2	170	240	410
2.3	170	230	400
2.5	185	230	415
2.7	186	215	401

Appendix B

Labeled DSC/TGA Traces

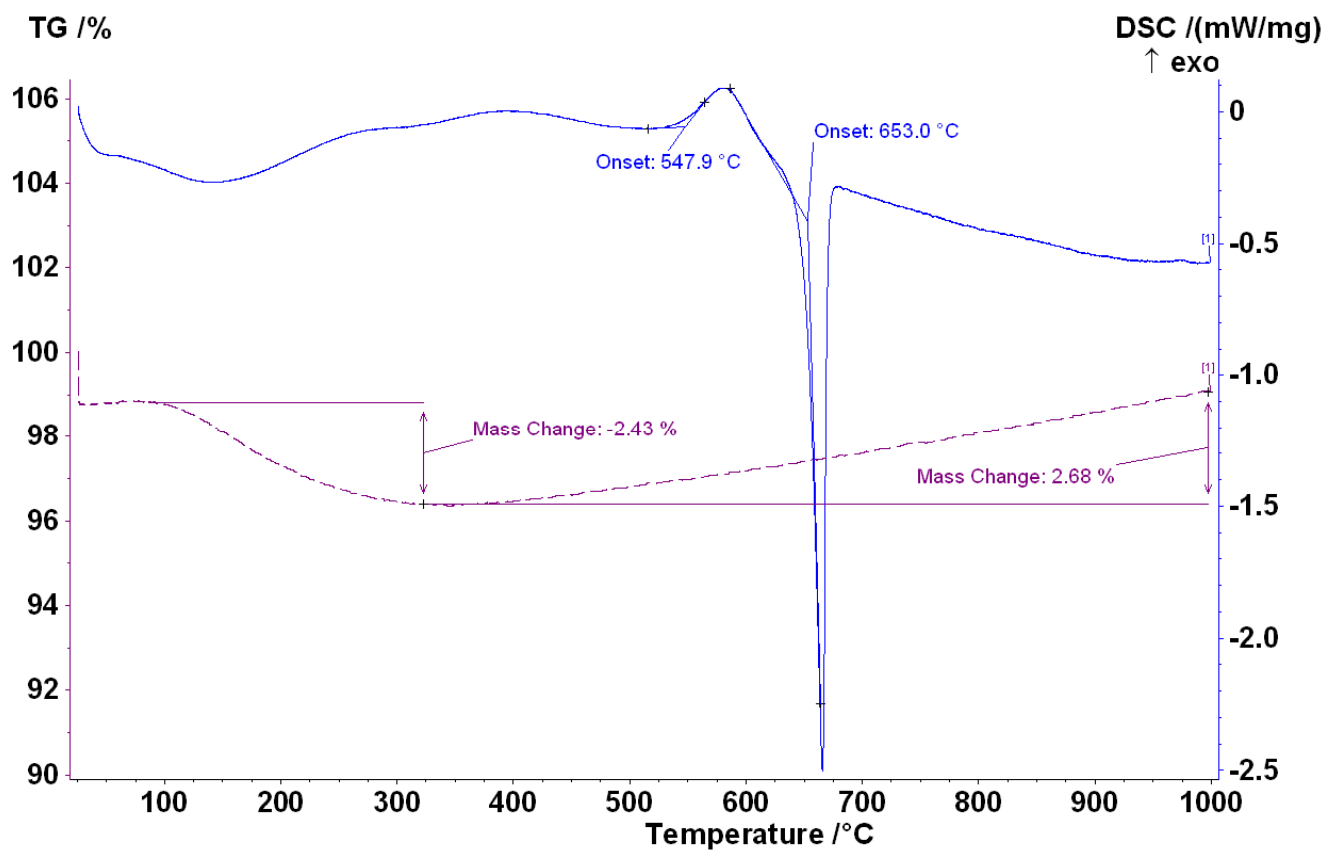


Figure 15. Labeled DSC/TGA trace of nm Al.

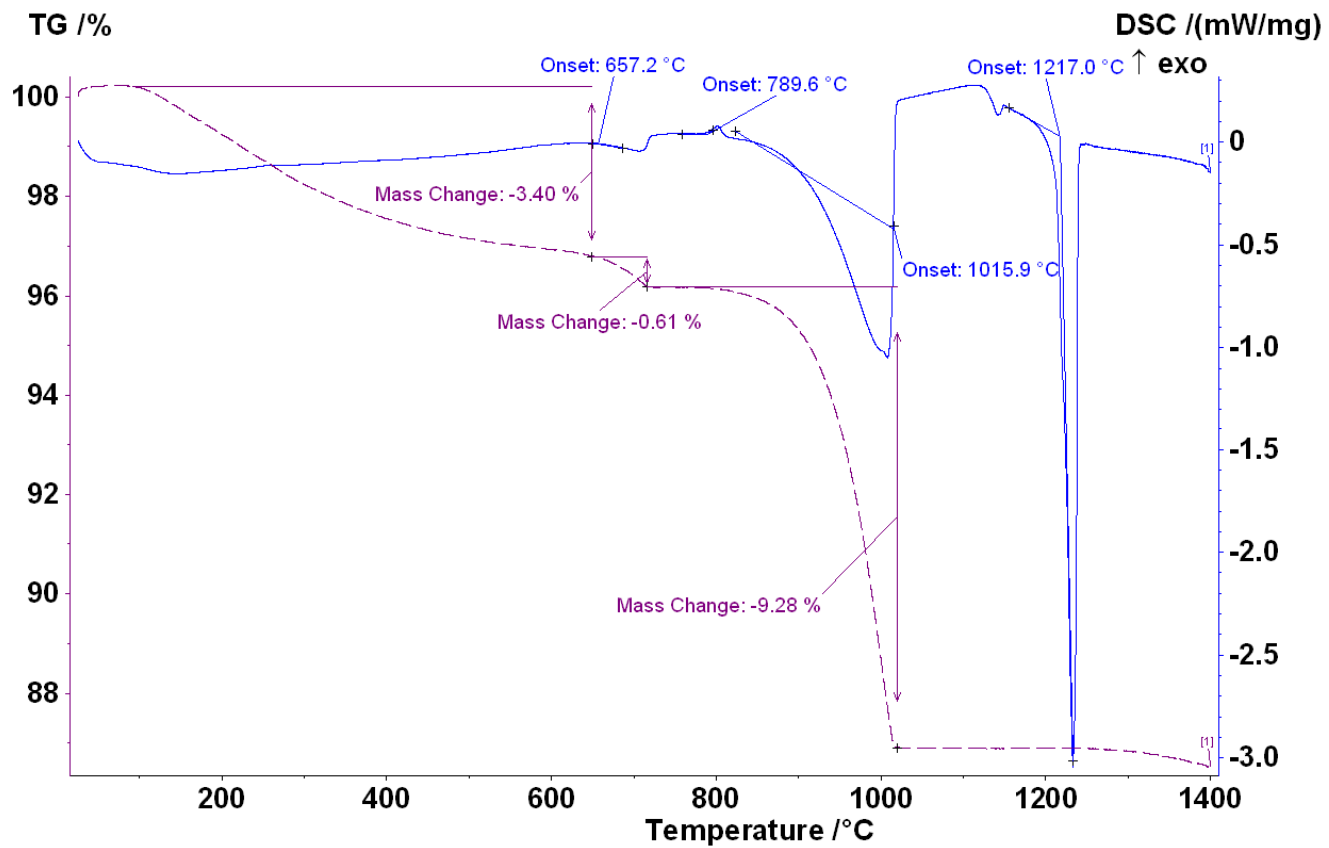


Figure 16. Labeled DSC/TGA trace of CuO.

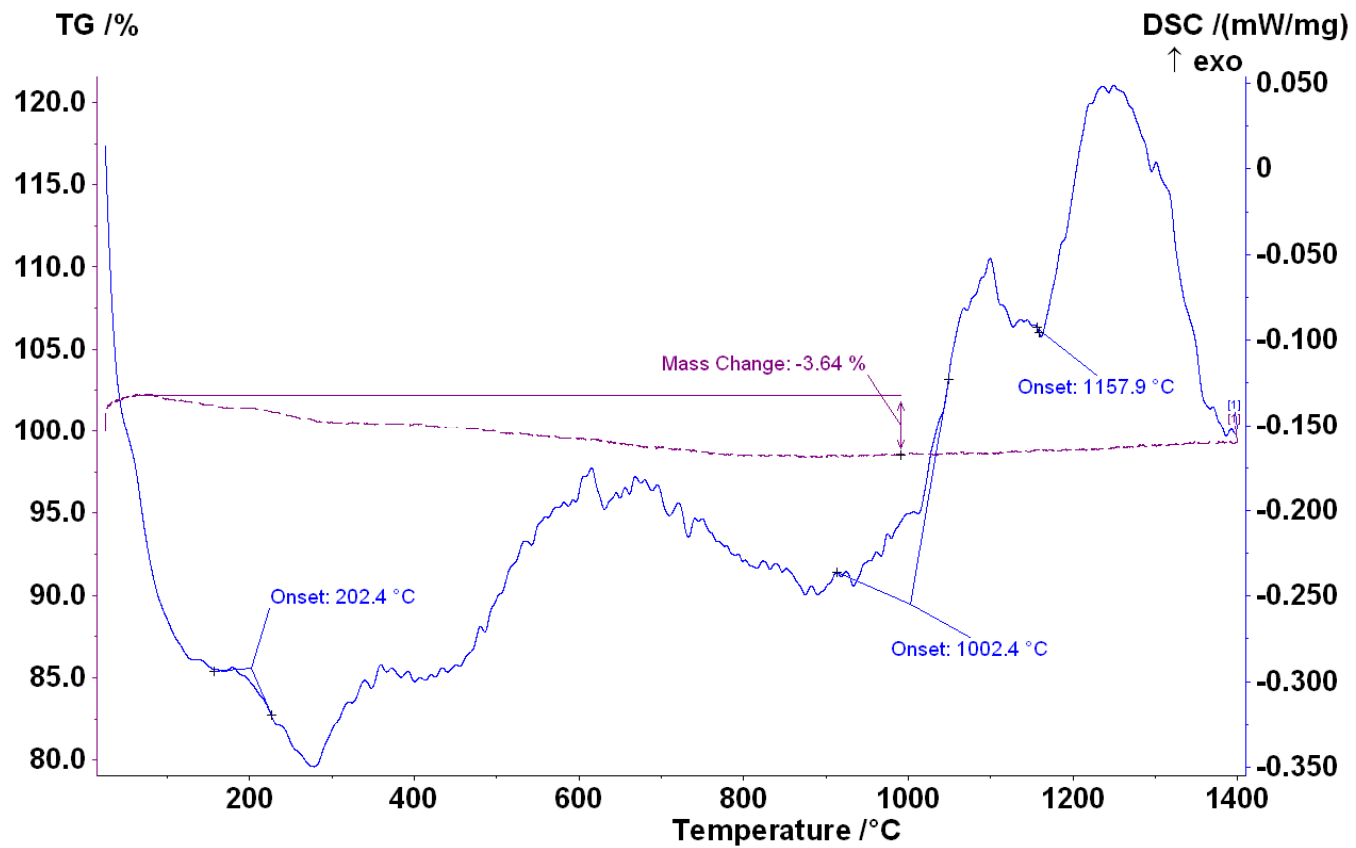


Figure 17. Labeled DSC/TGA trace of NiO.

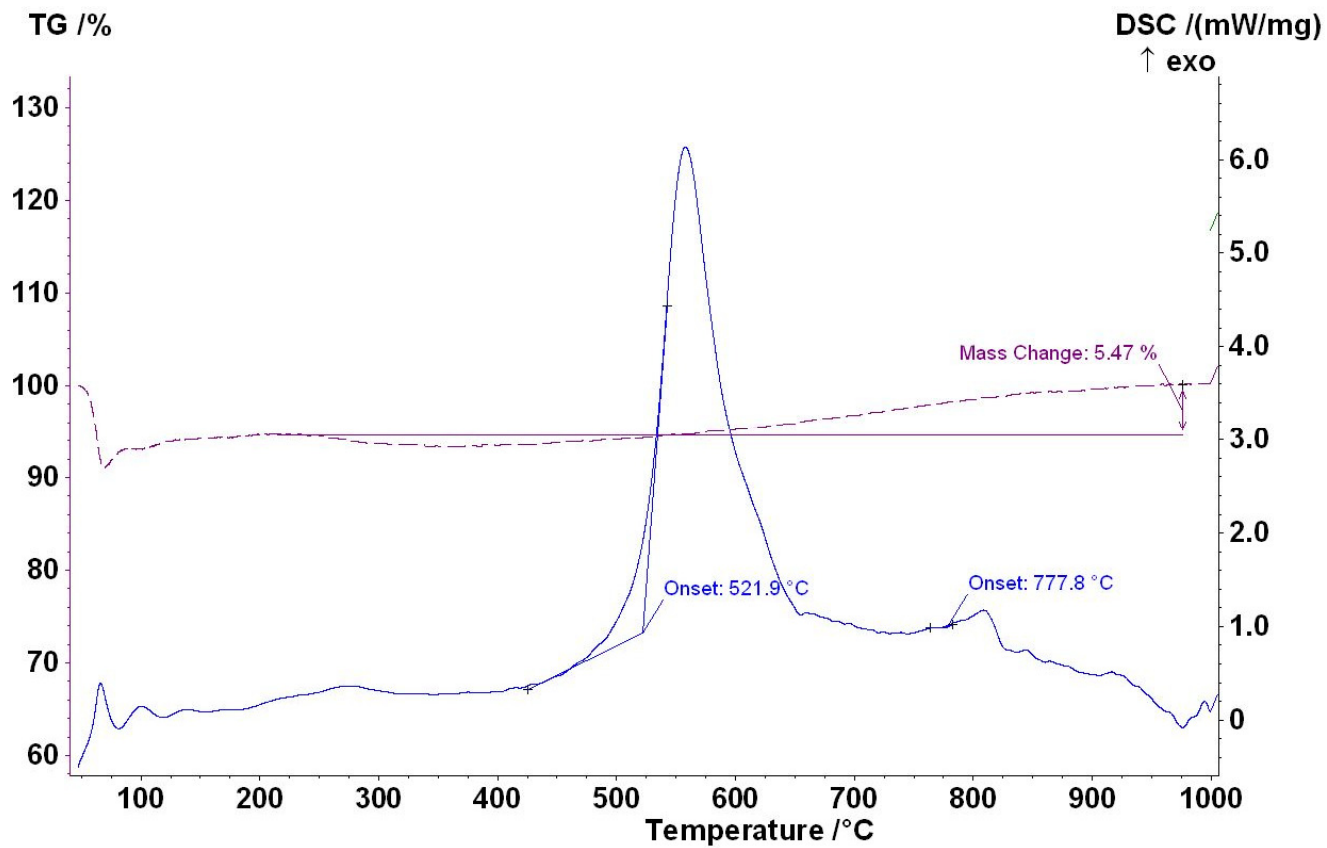


Figure 18. Labeled DSC/TGA trace of nm Al + CuO.

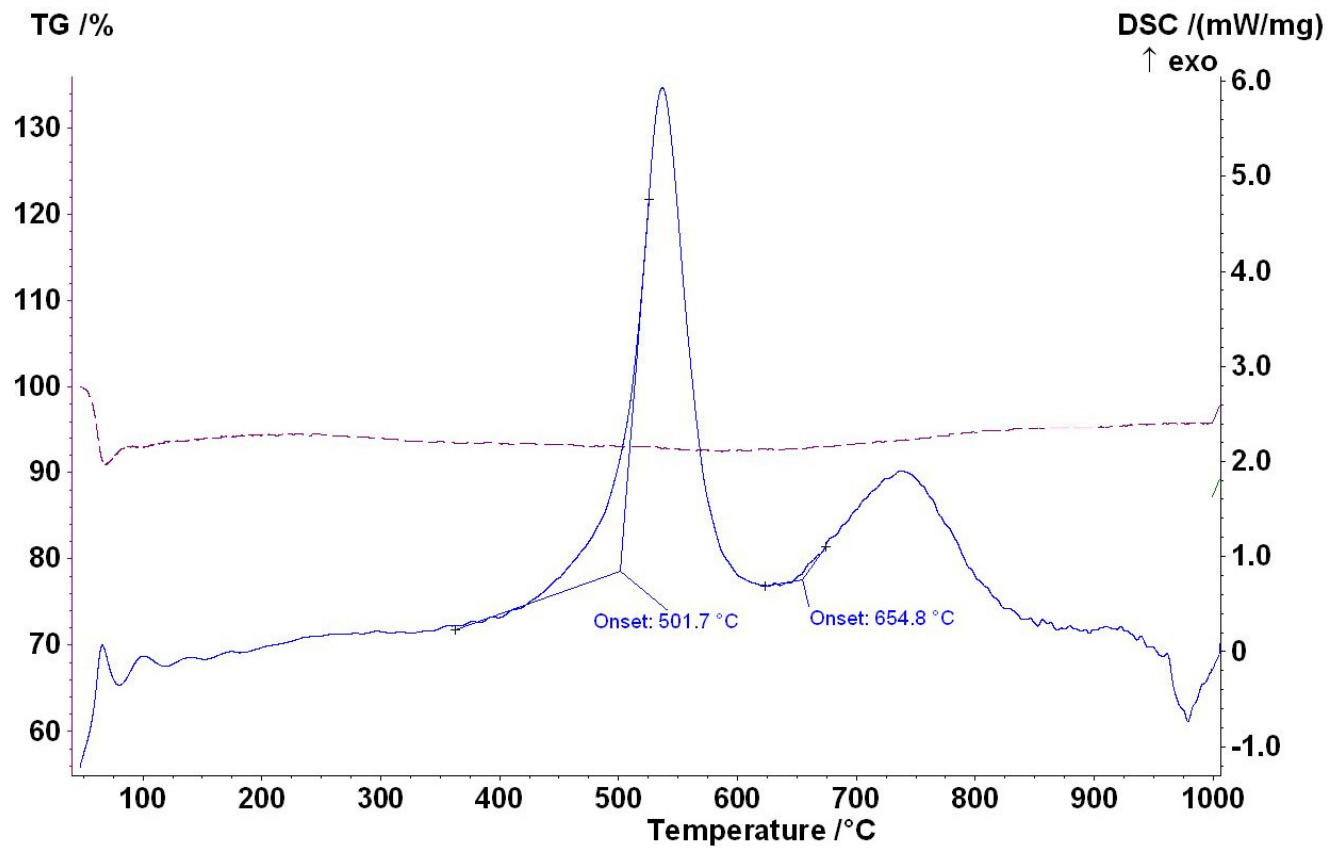


Figure 19. Labeled DSC/TGA trace of nm Al + NiO.

PERMISSION TO COPY

In presenting this thesis in partial fulfillment of the requirements for a master's degree at Texas Tech University or Texas Tech University Health Sciences Center, I agree that the Library and my major department shall make it freely available for research purposes. Permission to copy this thesis for scholarly purposes may be granted by the Director of the Library or my major professor. It is understood that any copying or publication of this thesis for financial gain shall not be allowed without my further written permission and that any user may be liable for copyright infringement.

Agree (Permission is granted.)

Steven Dean
Student Signature

October 29, 2008
Date

Disagree (Permission is not granted.)

Student Signature

Date